Source Apportionment and Macro Tracer: integration of independent methods for quantification of Woody Biomass Burning contribution to PM_{10}

Milena Stracquadanio, Ettore Petralia*, Massimo Berico, Teresa M.G. La Torretta, Antonella Malaguti, Mihaela Mircea, Maurizio Gualtieri, Luisella Ciancarella

ENEA, National Agency for New technologies, Energy and Sustainable Economic Development, Laboratory of Atmospheric Pollution, via Martiri di Monte Sole 4, 40129 Bologna, Italy

* Corresponding author.
E-mail address: ettore.petralia@enea.it (E. Petralia).

Supplementary material

Chemical composition of the other sources profiles

Fresh Marine aerosol. Fresh Marine aerosol is quite clear, with the sharp presence of Cl^- (81.3 %), Na^+ (54.2 %) and Mg^{2+} (49.6 %), markers recognised in literature for that source (Pio *et al.*, 1996; Belis *et al.*, 2013). The ratios Ca^{2+}/Na^+ (0.05) and Mg^{2+}/Na^+ (0.13) are in agreement to those reported in literature for that source (Millero, 1973; Waked *et al.*, 2014) even for Mediterranean basin (Calzolai *et al.*, 2015). The contribution to Σspec is 14.7 % while the contribution of PM_{10_comp} attributable to Fresh Marine aerosol is 13.0 %. The difference between Σspec and the PM_{10_comp}, as reported in Fig. 5, is well expected since the mass reconstructed from Σspec is lacking the water content related to fresh sea salt particles. Furthermore recent publications (Li *et al.*, 2018 and Fourtziou *et al.,* 2017) showed that species normally related only to sea salt particles may be related to other sources increasing the uncertainty of the mass reconstructed only from the chemical species.

Soil Dust. Prevailing species in Soil dust source are Si (72.1 %), Al (65.5 %), Fe (37.0 %), Ti (53.1 %), Mn (21.7 %) typical soil components (Querol *et al.*, 2002). In particular the Al/Si and Si/Al ratios are 0.48 and 2.06, comparable with others in literature for central Mediterranean area (Blanco *et al.*, 2003; Marconi *et al.*, 2014). The contribution to Σspec is 5.4 % while the contribution of PM_{10_comp} attributable to Soil dust is 11.5 %.

Vehicular traffic emission. The combined presence of EC (21.3 %), Ca^{2+} (13.8 %), Ti (10.6 %), Mn (27.6 %), Fe (33.9 %), Cu (23.8 %), Zn (23.7 %) suggests that this factor could represent the Vehicular traffic, with both traffic exhaust emissions and road-traffic related resuspension. In particular Cu, Zn and Fe are tracers for brakes and tires abrasion (Querol *et al*., 2007; Amato *et al*., 2009; Johansson *et al*., 2009; Minguillon *et al*., 2012; Minguillon *et al*., 2014; Megido *et al*., 2016) and Mn is also present as additive in gasoline (being included in traffic profile by Mansha *et al*., 2012 and Minguillon *et al*., 2014). Indeed Vehicular traffic emission is not so immediately to be isolated as pure factor, since it represents a minor emission source (Almeida *et al*., 2005; Waked *et al*., 2014) mainly in sub-urban sites; in fact the enrichment from simultaneous presence in that factor of V (11.1 %) and Ni (17.5 %) (oil combustion/industrial origin) is rather attributable to industrial/port activity reported for the wide area. The contribution to Σspec is 5.4 % while the contribution of PM_{10_comp} attributable to Vehicular traffic emission is 5.1 %.

Industrial/Port activity. That factor shows the high percent contribution of Mn (30.2 %) and Zn (48.7 %), to which couple of elements Marcazzan *et al*. (2003) and Bernardoni *et al*. (2011) connected the Industrial activity source, along with Cu (54.8 %) (Minguillon *et al*., 2014); as is done by Reche *et al*. (2012) within a research on $PM_{2.5}$. Besides other elements belonging to that factor are OC (15.5 %) and K^+ (10.2 %) related to combustion processes, and V (21.7 %) and Ni (55.9 %) related to oil combustion at harbour activity (Querol *et al*., 2009; Waked *et al*., 2014). The contribution to Σspec is 7.8 % while the contribution of PM_{10_comp} attributable to Industrial/port activity is 10.2 %.

Re-suspended Dust. This factor is similar to that Soil dust but it shows prevailing Ca^{2+} species (46.5 %), along with Al (17.2 %), Si (25.7 %), Ti (18.5 %), Fe (15.1 %) and Zn (6.4 %) elements re-entered into suspension by vehicular traffic. The high level of Ca^{2+} in that source may also be connected with construction works as reported by Kim *et al*. (2003), Bernardoni *et al*. (2011) and supposed by Srimuruganandam &Shiva Nagendra (2012), with an Al/Si ratio (0.36) similar to that found by Bernardoni *et al*. (2011). A dominant role was also played by a sand transport phenomenon occurred from the South during the measurements. The contribution to Σspec is 5.0 % while the contribution of PM_{10_comp} attributable to Resuspended dust is 3.3 %.

Nitrate-rich Secondary aerosol. This factor is characterised mostly by NO_3^- (52.2 %) together with NH_4^+ (51.2 %), clear tracers of Nitrate-rich Secondary aerosol. The quite high presence of EC (24.3 %), OC (23.1 %) and K^+ (22.1 %) within the factor can suggest a certain enrichment from combustion processes. The contribution to Σspec is 19.7 % while the contribution of PM_{10_comp} attributable to Nitrate-rich Secondary aerosol is 20.3 %.

Sulfate-rich Secondary aerosol. The simultaneous presence of SO_4^{2-} (37.9 %) and NH_4^+ (40.9 %) is the signature for Sulfate-rich Secondary aerosol, related to regional background and long-range transport. The contribution to Σspec is 9.4 % while the contribution of PM_{10_comp} attributable to Sulfate-rich Secondary aerosol is 8.2 %.

Aged Marine aerosol. The ninth factor is the so-called Aged Marine aerosol, defined as such because differently than the Fresh Marine aerosol presents no Cl^- (which comes to be lost rapidly) (Nicolás *et al*., 2009) but only Na^+ (31.3 %) and Mg^{2+} (30.1 %). This factor is mixed with secondary components from anthropogenic activities (Minguillon *et al*., 2014; Waked *et al*., 2014), as evidenced by NO_3^- (24.8 %) and SO_4^{2-} (32.9 %) carried by the wind at the time of air masses displacement. The contribution to Σspec is 10.7 % while the contribution of PM_{10_comp} attributable to Aged Marine aerosol is 6.5 %.

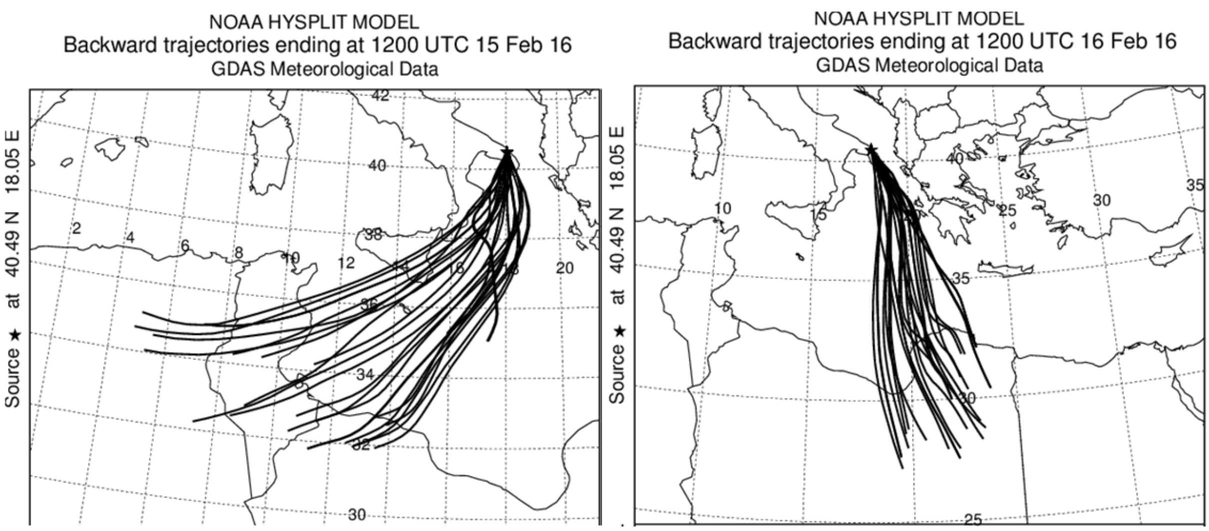

Figure S1. Back trajectories for the study area showing air masses occurring the 15th and 16th February 2016 (https://www.arl.noaa.gov/)

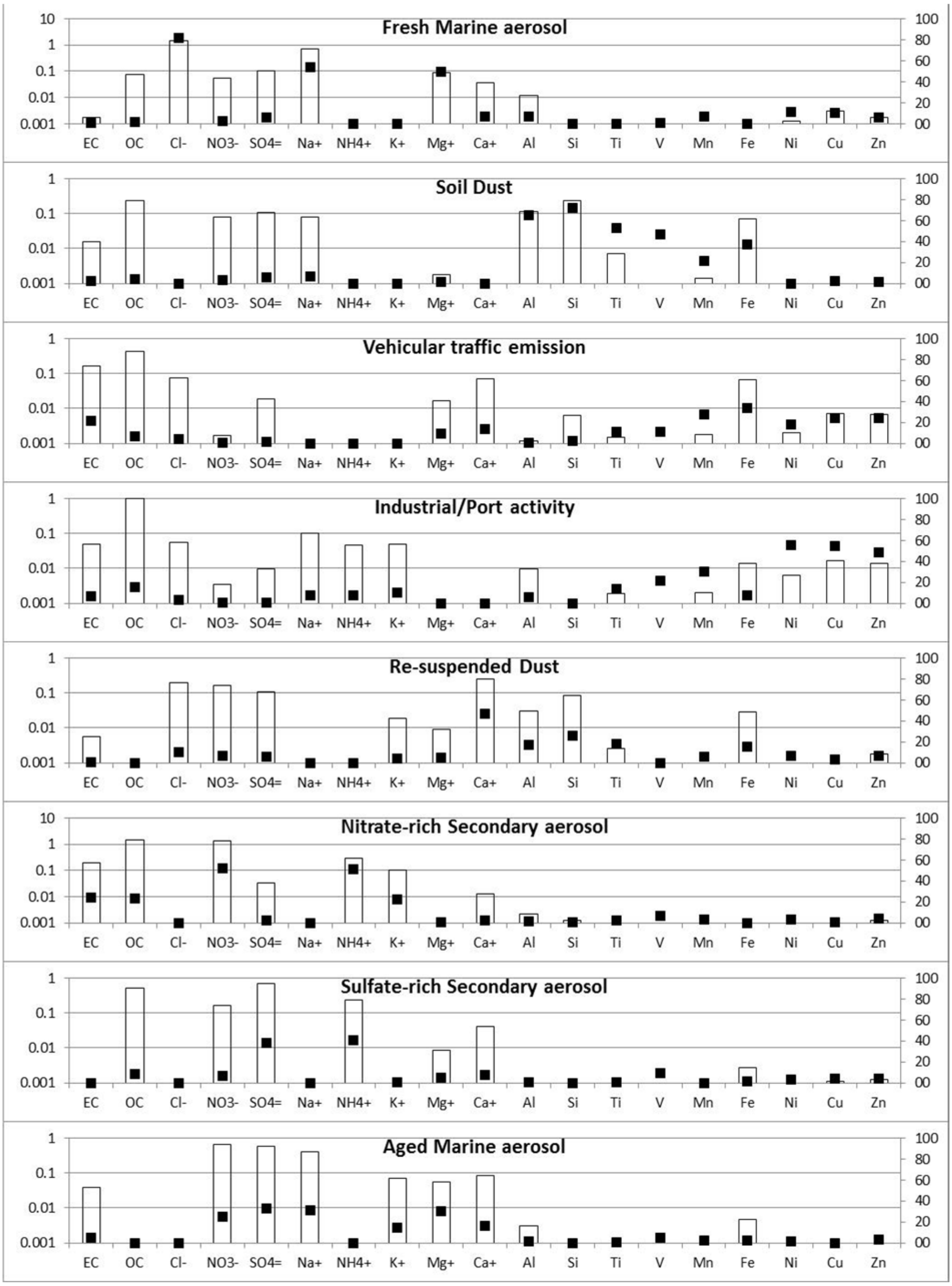

Figure S2. Factor profiles obtained from PMF analysis; Vertical bars (principal y-axis): mass concentration (μg m^{-3}) of the single element in the factor; Black squares (secondary y-axis): % contribution of the single element in the factor over the totality of factors

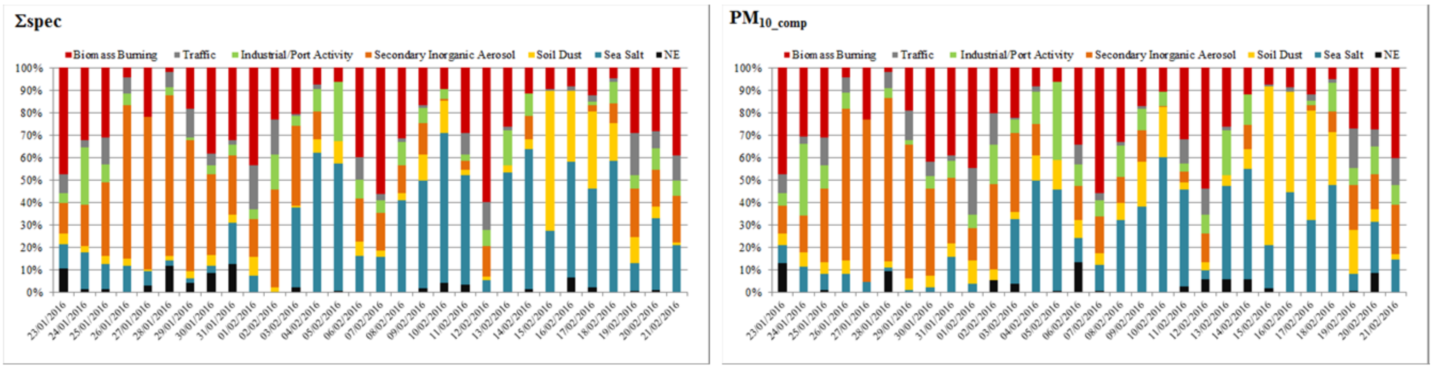

Figure S3. Daily percentage sources contribution for ∑spec (a) and for parameter PM10_comp (b)

Table S1. Metals and trace elements Method Detecion Limit (MDL) and combined relative standard uncertainty (ε_R)

	Na	**Mg**	**Al**	**Si**	**K**	**Cu**	**Ca**	**Ti**	**V**	**Cr**	**Mn**
MDL $_{\mu g\ m^{-3}}$	0.0098	0.016	0.0011	0.00035	0.077	0.0010	0.0033	0.0016	0.00012	0.00036	0.0013
ε_R	0.04	0.04	0.04	0.06	0.04	0.09	0.05	0.09	0.09	0.07	0.09
	Fe	**Co**	**Ni**	**Zn**	**As**	**Rb**	**Sb**	**Ba**	**W**	**S**	**Ce**
MDL $_{\mu g\ m^{-3}}$	0.0093	0.000011	0.00046	0.0013	0.000059	0.00013	0.00038	0.0027	0.0057	0.00022	0.00013
ε_R	0.05	0.09	0.11	0.10	0.04	0.08	0.06	0.12	0.10	0.03	0.09

Table S2. Descriptive statistics for the measured parameters

Sampling Site	PM_{10}	Cl^-	NO_3^-	SO_4^{2-}	Na^+	NH_4^+	K+	Mg^{2+}	Ca^{2+}	Al	Si	Ti	V	Mn	Fe	Ni	Cu	Zn	EC	OC
	$\mu g\ m^{-3}$	$\mu g\ m^{-3}$	$\mu g\ m^{-3}$	$\mu g\ m^{-3}$	$\mu g\ m^{-3}$	$\mu g\ m^{-3}$	$\mu g\ m^{-3}$	$\mu g\ m^{-3}$	$\mu g\ m^{-3}$	$\mu g\ m^{-3}$	$\mu g\ m^{-3}$	$\mu g\ m^{-3}$	$\mu g\ m^{-3}$	$\mu g\ m^{-3}$	$\mu g\ m^{-3}$	$\mu g\ m^{-3}$	$\mu g\ m^{-3}$	$\mu g\ m^{-3}$	$\mu gC\ m^{-3}$	$\mu gC\ m^{-3}$
Cisternino																				
Mean	24	1.8	2.6	1.7	1.2	0.60	0.47	0.17	0.58	0.17	0.33	0.014	0.00091	0.0059	0.18	0.011	0.027	0.027	0.65	5.3
Median	19	0.64	1.6	1.4	0.75	0.26	0.33	0.11	0.37	0.07	0.10	0.0073	0.00068	0.0051	0.13	0.010	0.026	0.026	0.51	3.8
SD	14	2.8	2.5	0.99	1.4	0.82	0.32	0.16	0.68	0.30	0.71	0.022	0.00085	0.0033	0.21	0.0023	0.0052	0.0057	0.48	3.8
25th Percentile	14	0.28	1.09	1.07	0.38	0.15	0.23	0.08	0.25	0.05	0.07	0.0057	0.00050	0.0041	0.09	0.009	0.024	0.023	0.24	2.2
75th Percentile	27	1.6	3.2	2.4	1.5	0.54	0.65	0.17	0.55	0.12	0.20	0.011	0.0010	0.0059	0.15	0.011	0.028	0.029	0.95	7.9
Min	9	0.13	0.63	0.62	0.18	0.01	0.11	0.05	0.18	0.03	0.03	0.00	0.00	0.0031	0.04	0.007	0.022	0.019	0.13	1.5
Max	51	12	11	4.8	6.1	3.1	1.4	0.71	3.0	1.5	3.6	0.11	0.0045	0.0206	1.1	0.020	0.051	0.041	1.7	15
Torchiarolo																				
Mean	32	2.3	3.0	2.0	1.5	0.98	0.62	0.22	0.61	0.21	0.42	0.017	0.0012	0.0080	0.25	0.012	0.034	0.030	1.09	8.3
Median	28	1.4	2.3	2.0	1.2	0.31	0.48	0.17	0.41	0.11	0.17	0.010	0.00093	0.0062	0.17	0.011	0.030	0.029	0.79	6.3
SD	13	2.6	2.2	0.90	1.2	1.54	0.34	0.15	0.53	0.33	0.77	0.022	0.00091	0.0048	0.23	0.006	0.021	0.014	0.75	5.3
25th Percentile	21	0.56	1.64	1.3	0.50	0.18	0.38	0.12	0.34	0.08	0.12	0.0080	0.00070	0.0052	0.13	0.009	0.026	0.024	0.49	4.5
75th Percentile	45	2.7	3.6	2.6	2.1	1.20	0.76	0.27	0.59	0.14	0.27	0.015	0.0016	0.0095	0.27	0.013	0.036	0.035	1.82	11
Min	17	0.27	0.75	0.72	0.12	0.00	0.21	0.074	0.14	0.00	0.00	0.00	0.00	0.00	0.00	0.00	0.00	0.00	0.18	2.2
Max	58	13	9.0	4.3	4.9	7.2	1.4	0.70	2.4	1.6	3.7	0.10	0.0039	0.0187	1.0	0.040	0.14	0.086	2.5	19

	PM_{10}	Cl^-	NO_3^-	SO_4^{2-}	Na^+	NH_4^+	K+	Mg^{2+}	Ca^{2+}	Al	Si	Ti	V	Mn	Fe	Ni	Cu	Zn	EC	OC
	$\mu g\ m^{-3}$	$\mu g\ m^{-3}$	$\mu g\ m^{-3}$	$\mu g\ m^{-3}$	$\mu g\ m^{-3}$	$\mu g\ m^{-3}$	$\mu g\ m^{-3}$	$\mu g\ m^{-3}$	$\mu g\ m^{-3}$	$\mu g\ m^{-3}$	$\mu g\ m^{-3}$	$\mu g\ m^{-3}$	$\mu g\ m^{-3}$	$\mu g\ m^{-3}$	$\mu g\ m^{-3}$	$\mu g\ m^{-3}$	$\mu g\ m^{-3}$	$\mu g\ m^{-3}$	$\mu gC\ m^{-3}$	$\mu gC\ m^{-3}$
Lendinuso																				
Mean	26	1.9	2.4	1.7	1.3	0.56	0.42	0.17	0.39	0.17	0.31	0.012	0.0010	0.0060	0.16	0.011	0.029	0.027	0.57	5.5
Median	22	1.2	2.0	1.6	0.89	0.33	0.32	0.13	0.26	0.09	0.13	0.009	0.0010	0.0052	0.11	0.010	0.028	0.025	0.41	3.3
SD	12	2.1	1.8	0.74	1.1	0.56	0.25	0.13	0.42	0.23	0.53	0.016	0.00072	0.0025	0.16	0.0024	0.0059	0.0059	0.48	4.5
25th Percentile	17	0.38	1.2	1.05	0.44	0.18	0.23	0.07	0.22	0.07	0.08	0.007	0.00057	0.0046	0.086	0.0094	0.026	0.023	0.24	2.4
75th Percentile	35	2.6	2.6	2.0	1.9	0.81	0.56	0.22	0.31	0.11	0.20	0.011	0.0012	0.0064	0.16	0.012	0.030	0.031	0.77	7.0
Min	11	0.16	0.52	0.78	0.13	0.022	0.068	0.036	0.13	0.044	0.046	0.00	0.00	0.0028	0.049	0.0077	0.021	0.019	0.033	1.1
Max	56	11	7.2	3.5	4.9	2.1	1.2	0.60	2.0	1.1	2.4	0.071	0.0032	0.0154	0.77	0.020	0.054	0.042	2.2	18

Table S3. ΣSpec and PM_{10_comp} sources percentage contribution to PM_{10}

	Biomass Burning		**Traffic**		**Secondary Inorganic Aerosol**		**Soil Dust**		**Sea Salt**		**Industrial/Port Activity**		**NE**	
	ΣSpec	**PM_{10_comp}**	ΣSpec	**PM_{10_comp}**	ΣSpec	**PM_{10_comp}**	ΣSpec	**PM_{10_comp}**	ΣSpec	**PM_{10_comp}**	ΣSpec	**PM_{10_comp}**	ΣSpec	**PM_{10_comp}**
	%	**%**	**%**	**%**	**%**	**%**	**%**	**%**	**%**	**%**	**%**	**%**	**%**	**%**
Mean	25	25	6.0	6.3	22	22	9.0	13	28	23	7.4	9.7	2.7	2.6
Median	25	25	3.1	3.1	16	15	4.1	6.2	20	16	5.8	7.5	1.3	0.29
SD	16	16	5.8	5.7	22	22	12.9	16	22	18	6.4	8.2	3.7	4.0
25th Percentile	10	11	1.5	1.7	8.9	9.0	2.9	4.9	11	7.6	4.0	5.5	0.11	0.00
75th Percentile	32	34	9.8	11	33	33	9.8	13	49	42	9.7	13	3.4	5.1
Min	1.9	1.9	0.081	0.09	0.89	0.1	0.78	2.5	2.0	0.86	1.3	1.7	0.11	0.0
Max	60	56	20	21	72	73	62	71	67	60	27	35	13	13

References

Almeida, S.M., Pio, C.A., Freitas, M.C., Reis, M.A., Trancoso, M.A., (2005). Source apportionment of fine and coarse particulate matter in a sub-urban area at the Western European Coast. *Atmos. Environ*., 39: 3127–3138.

Amato, F., Pandolfi, M., Viana, M., Querol, X., Alastuey, A., Moreno, T, (2009). Spatial and chemical patterns of PM_{10} in road dust deposited in urban environment. *Atmos. Environ*., 43: 1650–1659.

Belis, C.A., Karagulian, F., Larsen, B.R., Hopke, P.K., (2013). Critical review and meta-analysis of ambient particulate matter source apportionment using receptor models in Europe, *Atmos. Environ*., 69: 94–108.

Bernardoni, V., Vecchi, R., Valli, G., Piazzalunga, A., Fermo, P., (2011). PM_{10} source apportionment in Milan (Italy) using time-resolved data. *Sci. Total Environ.*, 409: 4788–4795.

Blanco, A., De Tomasi, F., Filippo, E., Manno, D., Perrone, M.R., Serra, A., Tafuro, A.M., Tepore, A., (2003). Characterization of African dust over southern Italy. *Atmos. Chem. Phys*., 3: 2147–2159.

Calzolai, G., Nava, S., Lucarelli, F., Chiari, M., Giannoni, M., Becagli, S., Traversi, R., Marconi, M., Frosini, D., Severi, M., Udisti, R., Di Sarra, A., Pace, G., Meloni, D., Bommarito, C., Monteleone, F., Anello, F., Sferlazzo, D.M., (2015). Characterization of PM_{10} sources in the central Mediterranean. *Atmos. Chem. Phys.*, 15: 13939–13955.

Fourtziou, L., Liakakou, E., Stavroulas, I., Theodosi, C., Zarmpas, P., Psiloglou, B., Mihalopoulos, N. (2017). Multi-tracer approach to characterize domestic wood burning in Athens (Greece) during wintertime. *Atmos. Environ*. 148: 89–101.

Johansson, C., Norman, M., Burman, L., (2009). Road traffic emission factors for heavy metals. *Atmos. Environ*., 43: 4681–4688.

Kim, E., Hopke, P.K., Edgerton, E.S., (2003). Source Identification of Atlanta Aerosol by Positive Matrix Factorization. *Air & Waste Manage. Assoc.*, 53:731–739.

Li, J., Chen, B., de la Campa, A. M. S., Alastuey, A., Querol, X., de la Rosa, J. D. (2018). 2005–2014 trends of PM10 source contributions in an industrialized area of southern Spain. *Environ. Pollut.*, *236*: 570–579.

Mansha, M., Ghauri, B., Rahman, S., Amman, A., (2012). Characterization and source apportionment of ambient air particulate matter ($PM_{2.5}$) in Karachi. *Sci. Total Environ.*, 425: 176–183.

Marcazzan, G.M., Ceriani, M., Valli, G., Vecchi, R., (2003). Source apportionment of PM_{10} and $PM_{2.5}$ in Milan (Italy) using receptor modelling. *Sci. Total Environ.*, 317: 137–147.

Marconi, M., Sferlazzo, D.M., Becagli, S., Bommarito, C., Calzolai, G., Chiari, M., Di Sarra, A., Ghedini, C., Gómez-Amo, J.L., Lucarelli, F., Meloni, D., Monteleone, F., Nava, S., Pace, G., Piacentino, S., Rugi, F., Severi, M., Traversi, R., Udisti, R., (2014). Saharan dust aerosol over the central Mediterranean Sea: PM_{10} chemical composition and concentration versus optical columnar measurements. *Atmos. Chem. Phys.*, 14: 2039–2054.

Megido, L., Negral, L., Castrillón, L., Marañón, E., Fernández-Nava, Y., Suárez-Peña, B., (2016). Traffic tracers in a suburban location in northern Spain: relationship between carbonaceous fraction and metals. *Environ. Sci. Pollut. Res*., 23:8669–8678.

Millero, F., (1973). Seawater – A test of multicomponent electrolyte solution theories. I. The apparent equivalent volume, expansibility, and compressibility of artificial seawater. *J. Solution. Chem*., 2: 1–22.

Minguillón, M.C., Querol, X., Baltensperger, U., Prévôt, A.S.H., (2012). Fine and coarse PM composition and sources in rural and urban sites in Switzerland: Local or regional pollution? *Sci. Total Environ.*, 427-428: 191–202.

Minguillón, M.C., Cirach, M., Hoek, G., Brunekreef, B., Tsai, M., De Hoogh, K., Jedynska, A., Kooter, I.M., Nieuwenhuijsen, M., Querol, X., (2014). Spatial variability of trace elements and sources for improved exposure assessment in Barcelona. *Atmos. Environ*., 89: 268-281.

Nicolás, J.F., Galindo, N., Yubero, E., Pastor, C., Esclapez, R., Crespo, J., (2009). Aerosol Inorganic Ions in a Semiarid Region on the Southeastern Spanish Mediterranean Coast. *Water Air Soil Pollut.*, 201:149–159.

Pio, C.A., Cerqueira, M.A., Castro, L.M., Salgueiro, M.L., (1996). Sulphur and nitrogen compounds in variable marine/continental air masses at the southwest European coast. *Atmos. Environ.*, 30: 3115–3127.

Querol, X., Alastuey, A., De la Rosa, J., Sánchez de la Campa, A., Plana, F., Ruiz, C.R., (2002). Source apportionment analysis of atmospheric particulates in an industrialised urban site in southwestern Spain. *Atmos. Environ.*, 36: 3113–3125.

Querol, X., Viana, M., Alastuey, A., Amato, F., Moreno, T., Castillo, S., Pey, J., De la Rosa, J., Sánchez de la Campa, A., Artíñano, B., Salvador, P., García Dos Santos, S., Fernández-Patier, R., Moreno-Grau, S., Negral, L., Minguillón, M.C., Monfort, E., Gil, J.I., Inza, A., Ortega, L.A., Santamaría, J.M., Zabalza, J., (2007). Source origin of trace elements in PM from regional background, urban and industrial sites of Spain. *Atmos. Environ.*, 41: 7219–7231.

Querol, X., Alastuey, A., Pey, J., Cusack, M., Pérez, N., Mihalopoulos, N., Theodosi, C., Gerasopoulos, E., Kubilay, N., Koçak, M., (2009). Variability in regional background aerosols within the Mediterranean. *Atmos. Chem. Phys.*, 9: 4575–4591.

Reche, C., Viana, M., Amato, F., Alastuey, A., Moreno, T., Hillamo, R., Teinilä, K., Saarnio, K., Seco, R., Peñuelas, J., Mohr, C., Prévôt, A.S.H., Querol, X., (2012). Biomass burning contributions to urban aerosols in a coastal Mediterranean City. *Sci. Total Environ.*, 427-428: 175–190.

Srimuruganandam, B., Shiva Nagendra, S.M., (2012). Application of positive matrix factorization in characterization of PM_{10} and $PM_{2.5}$ emission sources at urban roadside. *Chemosphere*, 88: 120–130.

Waked, A., Favez, O., Alleman, L.Y., Piot, C., Petit, J.-E., Delaunay, T., Verlinden, E., Golly, B., Besombes, J.-L., Jaffrezo, J.-L., Leoz-Garziandia, E., (2014). Source apportionment of PM_{10} in a north-western Europe regional urban background site (Lens, France) using positive matrix factorization and including primary biogenic emissions. *Atmos. Chem. Phys.*, 14: 3325–3346.